Earth and Planetary Science Letters 295 (2010) 177–186

Contents lists available at ScienceDirect

Earth and Planetary Science Letters

journal homepage: www.elsevier.com/locate/epsl

Turbulent mixing of metal and silicate during planet accretion — And interpretation of the Hf–W chronometer

Tais W. Dahl [a,*], David J. Stevenson [b]

[a] Planet and Geophysics, Niels Bohr Institute, Juliane Maries Vej 30, DK-2100 Copenhagen OE, Denmark
[b] Division of Geological and Planetary Science, California Institute of Technology 150-21, Pasadena, CA 91125, USA

ARTICLE INFO

Article history:
Received 26 October 2009
Received in revised form 16 February 2010
Accepted 24 March 2010
Available online 10 May 2010

Editor: T. Spohn

Keywords:
core formation
tungsten isotopes
siderophile elements
turbulence
Earth
Moon

ABSTRACT

In the current view of planet formation, the final assembly of the Earth involved giant collisions between proto-planets (>1000 km radius), with the Moon formed as a result of one such impact. At this stage the colliding bodies had likely differentiated into a metallic core surrounded by a silicate mantle. During the Moon-forming impact, nearly all metal sank into the Earth's core. We investigate to what extent large self-gravitating iron cores can mix with surrounding silicate and how this influences the short-lived chronometer, Hf–W, used to infer the age of the Moon. We present fluid dynamical models of turbulent mixing in fully liquid systems, attempting to place constraints on the degree of mixing. Erosion of sinking cores driven by Rayleigh–Taylor instability does lead to intimate mixing and equilibration, but large blobs (>10 km diameter) do not emulsify entirely. Emulsification is enhanced if most of the accreting metal cores deform into thin structures during descent through the Earth's mantle. Yet, only 1–20% of Earth's core would equilibrate with silicate during Earth's accretion. The initial speed of the impactor is of little importance. We proceed to evaluate the mixing potential for shear instabilities where silicate entrainment across vertical walls causes mixing. The turbulent structure indicates that vortices remain at the largest scale and do not mix to centimeter length scale, where diffusion operates and isotopes can equilibrate. Thus, incomplete emulsification and equilibration of accreting iron cores is likely to occur.

The extent of metal–silicate equilibration provides key information for interpretation of siderophile budgets and the timing of core formation using the Hf–W chronometer. The time scale of core formation derived from the Hf–W chronometer is usually tied to the last major metal–silicate re-equilibration, believed to coincide with time of the Moon-forming impact. However, we show that large cores have limited ability to reset the Hf–W system in the silicate Earth. Excess ^{182}W in bulk silicate Earth is more sensitive to early core formation processes than to radiogenic ingrowth after the last giant impact.

1. Introduction

The timing and style of the Earth's origin is constrained by a combination of numerical simulations and geochemical measures. In general the two approaches now seem to converge on late formation of the Moon at 4.50–4.45 Ga (Tera, 1974; Porcelli et al., 2001; Allegre et al., 2008). This event was probably also the last giant impact on Proto-Earth.

The formation of planets from a protoplanetary disk of dust and gas occurs in four stages: 1) formation of grains <0.01 m, which 2) clump together by turbulent motion to produce ~1 km bodies (Weidenschilling, 2000). Then, 3) run-away growth produces planetesimals of Mercury to Mars size over a short time scale of 0.1–1 Myrs (Kortenkamp et al., 2001; Chambers, 2004) 4). The late stages of planet accretion involve collisions between proto-planets and large bodies of the size of Mars on a ~10–100 Myr time scale (Chambers, 2004; O'Brien et al., 2006; Ogihara et al., 2007). It is currently believed that the proto-Earth suffered from the largest impact late in the accretion process, when ~80% or 90% of its mass had accumulated. This event led to the formation of the Moon. Isotopic evidence from meteorites reveals that core formation is fast (~1 Myrs) in some small (10 km) bodies (Chen and Wasserburg, 1996; Lee and Halliday, 1996; Markowski et al., 2006). The lack of metallic iron in the Moon (<3 wt.%, Earth: 32 wt.%) is attributed to the prior differentiation of both projectile and target, and the indication from numerical simulations is that the source material for the Moon primarily comes from the mantle of the projectile. The core of the projectile merges quickly with the core of Proto-Earth and this process is accordingly an important part of core formation in Earth. It is thought likely that the precursor bodies to Earth formation also possessed cores that formed very early.

In the last decade, Hf–W chronometry has been used to constrain the timing of the Moon forming impact by assuming this event to have significant importance for the siderophile budgets in Earth's mantle (Halliday et al., 1996; Harper and Jacobsen, 1996; Halliday and Lee,

* Corresponding author. Present address: Department of Organismic and Evolutionary Biology, Harvard University, 26 Oxford St, Cambridge, MA 02138, USA. Tel.: +1 617 495 7602; fax: +1 617 495 5667.
E-mail address: tdahl@fas.harvard.edu (T.W. Dahl).

0012-821X/$ – see front matter © 2010 Elsevier B.V. All rights reserved.
doi:10.1016/j.epsl.2010.03.038

1999; Kleine et al., 2002; Schoenberg et al., 2002; Yin et al., 2002; Halliday, 2004; Jacobsen, 2005; Kleine et al., 2005a; Wood and Halliday, 2005; Touboul et al., 2007; Kleine et al., 2009).

Measurements of W isotopes in lunar metals provide key evidence for the isolation of the Moon from the Earth occurring late in the accretion history (Kleine et al., 2005a), and recent data (Touboul et al., 2007) show that the $^{182}W/^{184}W$ of bulk silicate Earth, lunar metals and silicates are indistinguishable. Therefore, the Moon and silicate Earth evolved separately after nearly all ^{182}Hf had decayed. Early Moon formation can be ruled out because of the stochastic nature of planet accretion and $^{182}W/^{184}W$ evolution in the Proto-planetary mantles that would likely result in distinguishable W isotopic compositions (Nimmo and Kleine, 2007).

The silicate Earth and Moon are enriched in radiogenic $^{182}W/^{184}W$ relative to the chondritic value by 1.9 ε_W units (parts per 10,000) (Kleine et al., 2002; Schoenberg et al., 2002; Yin et al., 2002). Preliminary interpretation argued for an early Moon forming event, at ~4.54 Ga or ~30 Myrs after crystallization calcium–aluminum rich inclusions (CAI) in chondrites, by assuming that the silicate Earth was reset to the chondritic value after the impact. Subsequent core formation was stalled and excess ^{182}W was produced by later ^{182}Hf in-growth. However, this assumes efficient equilibration of siderophile W in the mantle with metallic Fe during the accretion event; basically every single W atom in the mantle must have seen metal during the event. In practice "seeing" means diffusive equilibration over some short distance. If one takes into account inefficient equilibration between metal and silicate (before transfer into Earth's core) during accretion, then the Moon could have formed later (Halliday, 2004).

What, then, is the significance of the $^{182}W/^{184}W$ excess in Bulk Silicate Earth (and the Moon) relative to chondrites? The ε_W evolution depends on how efficiently mantle W equilibrates with metallic Fe. We present fluid dynamical models for the degree of equilibration between metal and silicate during impact-driven planet accretion that suggest inability of giant cores to emulsify to a length scale where isotopes and elements can equilibrate. It allows us to assess Hf–W resetting in bulk silicate Earth after a single giant impact.

1.1. Core formation by impact driven accretion

Giant impacts are traumatic: severe distortion results both from direct material contact (shocks and pressure gradients) and from the action of gravity (Keplerian shear). Dynamical simulations using Smoothed-Particle Hydrodynamics (SPH), a code where impacting bodies are represented by a finite number of smooth particles (Cameron and Benz, 1991), provide a framework for the physical parameter space, e.g. the inclination of the impact (~45°), impact speed (9.3 km/s ~ escape velocity) and very high temperatures well above the melting point for metals and silicate (Canup, 2004), consistent with previous results (Davies, 1985; Melosh, 1990; Tonks and Melosh, 1993). Both projectile and target are likely to be liquid after such an impact, although part of the target material may remain solid (as suggested by Tonks and Melosh) well away from the direct effect of the impact. This likelihood is reduced if the pre-impact target is close to solidus conditions.

The primary differentiation of Earth is between the core and the mantle, and the disposition of elements between these reservoirs is central to our understanding of the dynamics and timing of Earth's accretion and early evolution. In order to make a connection between what we measure (e.g., in mantle rocks) and these formative processes, we need to know whether it was possible to equilibrate the core and mantle chemically and thermally. When did the last equilibration take place and what were the conditions in which it took place? Since giant impacts involve large fractions of the Earth forming material and may have occurred late in the accretion history, it is important to know whether equilibration might have occurred in their immediate aftermath.

Simulations give the impression of some "mixing" in the sense that particles of iron and silicate can become intermingled (Canup, 2004). However, it is a fallacy to suppose that the simulations guarantee or even suggest that mixing occurs down to the scales where chemical or thermal equilibration can act. There are two essential points that one must recognize when thinking about this issue. First, the characteristic dynamic timescale for the immediate post-impact evolution is only hours for large blobs. Many simulations show that iron from the projectile can reach the core of Proto-Earth during this period. In this time τ_{dyn}, compositional diffusion in a liquid can proceed a distance of order $(D\tau_{dyn})^{1/2} \sim 0.01$ m, where $D \sim 10^{-8}$ m^2/s is a typical diffusivity (all parameter values used for this study are summarized in SM-Table A1 in the Supplementary Material). This distance is about seven orders of magnitude below the resolution of the numerical simulations. Equally important, the existence of disruption and shearing at scales of hundreds to thousands of kilometers does not *automatically* imply comparable shearing and disruption at scales seven orders of magnitude smaller. Existing numerical simulations are not capable of addressing this issue and should not even be used to intuit the outcome.

Earlier models for the extent of mixing between metals and silicates during planet accretion focus on the magma ocean environment of core formation (Stevenson, 1990), overturning in a magma ocean (Sasaki and Abe, 2007) and core formation by drainage from large metal diapirs (Golabek et al., 2008). Efficient equilibration may occur for small metal droplets with internal circulation settling in a magma ocean. Iron spheres with a diameter <0.2 m can equilibrate in a deep magma ocean (Rubie et al., 2003; Sasaki and Abe, 2007). However, at larger length scales surface tension and viscosity are indeed negligible: The length scale relevant for surface tension competing with gravity is $L_{ST} \sim (\gamma/\Delta\rho g)^{1/2} \approx 5 \cdot 10^{-3}$ m (Chandrasekhar, 1961a) and viscosity modifies the growth of Rayleigh–Taylor instability below $L_{visc} \sim (\nu^2/Ag)^{1/3} \approx 10^{-3}$ m (Chandrasekhar, 1961b). In the absence of internal circulation a free particle can diffuse ~0.01 m in a silicate melt during the ~1 h time frame an iron core settles to the base of a maximal magma ocean (~3000 km).

Here, we explore the mixing in fully liquid systems. In systems where there is a shallow magma ocean bounded below by solid or a magma pool (as in some of the models discussed by Tonks and Melosh (1993)) the processes we discuss here still work in the fully liquid part of the system but fail completely in the solid part. The reason is that the solid (or mostly solid) medium has a viscosity that is typically ten to twenty orders of magnitude larger than for a melt and the Rayleigh–Taylor instability is then only large scale and can be visualized as large diapirs or plumes descending to the core, as in Stevenson (1990). In that limit, diffusive equilibration between solid silicates and iron is strongly suppressed by the very low diffusivity within solids and there is strong disequilibrium despite the longer timescale of core formation. In effect, the radiogenic ingrowth of tungsten in the deep solid part of the mantle has no opportunity to encounter liquid iron with which it can equilibrate. However, we are not considering here yet another possibility: percolative equilibration which would allow siderophiles to equilibrate with core forming liquid even in a system that is not mostly molten. We focus on the large-scale motions of iron and silicate fluids at all length scales up to the ~2000 km giant cores which settled into the Earth's core during final accretion. At this scale viscous forces and surface tension are indeed negligible. Hence, iron and silicate can be considered as inviscid, immiscible fluids. We suggest turbulent emulsification is responsible for breaking the cores down to sub-centimeter scale at which energy dissipates by droplet formation and viscous forces. At this scale, the results of (Rubie et al., 2003) predict fast equilibration.

2. Turbulent mixing during impact driven accretion

Our analysis considers the efficiency of emulsification of iron metal in silicate down to centimeter scale during and immediately an impact. We suggest emulsification is caused by hydrodynamic instabilities at the iron–silicate boundary. These are Rayleigh–Taylor (RT) and Kelvin–Helmholtz (KH) instabilities. The RT instability arises from the different pressure gradients on each side of a compositional boundary, but can be thought of

as buoyancy driven when the fluid acceleration is small compared to gravity. A special case of RT, known as the Richtmyer–Meshkov instability, arises during the passage of a shock wave across the interface between two fluids, but is limited in its effect by the short duration of large local pressure gradients. New experimental studies shed light on this process (Jacobsen et al., 2008; Tschauner et al., 2005; Petaev et al., 2008. The KH instability is driven by large-scale shear that could arise either through large-scale buoyancy driven flow or from the large scale deformation flow arising from the impact or from Keplerian shear. Our analysis suggests that RT is of greatest importance because it allows the rapid development of small-scale disturbances when the viscosity is low, as it will be at high temperature when both the iron and the silicate are liquid. We recognize, however, that the system of interest is not simply divided into RT and KH style of instability; there will in reality be some mixing of the processes (discussed further below). KH may feed the scales on which RT can act by stretching fluid elements (increasing their surface area).

2.1. Rayleigh–Taylor instability and turbulent structure

Rayleigh–Taylor instability is driven by a difference in pressure gradients between two fluids. In the special case of non-accelerated fluids separated by a horizontal boundary, the two pressure gradients are hydrostatic and their difference arises from the difference in fluid densities. RT instability is then simply the consequence of a dense fluid resting on a less dense fluid, and the boundary develops undulations of growing amplitude as gravitational energy is released and the dense fluid penetrates into the less dense fluid. One could alternatively imagine an initially stable arrangement of two fluids (light fluid on top of dense fluid), suddenly accelerated from rest (opposite to gravity).

When a system is RT-unstable, a small disturbance of the interface grows exponentially in amplitude, until nonlinearity takes over. A mixed zone develops; growing thicker with time, see Fig. 1A–D. The nonlinearity is expressed as turbulence, with a broad spectrum of scales of motion. The largest scale is comparable to the thickness of the region and the smallest scale is determined by viscosity or perhaps surface tension. Dalziel et al. (1999) carried out both laboratory and computer experiments to study the case of miscible fluids (water layers of different salinity) with an initially horizontal unstable interface. They found that the energy spectrum of RT-turbulence satisfies the Kolmogorov scaling law, $E(k) \propto k^{-5/3}$ where $1/k$ is the characteristic vortex length scale (Tennekes and Lumley, 1972). The $-5/3$ power law is consistent with fast shedding of large eddies into smaller eddies, known as the *Kolmogorov cascade.* This quasi-steady state turbulent cascade is set up in a time scale that is fast compared to the large-scale dynamical time scales. Energy primarily goes into larger eddies from which smaller eddies are shed. The kinetic energy is dissipated by viscous forces or droplet formation when the eddy size is comparable to Kolmogorov microscale of length (Tennekes and Lumley, 1972) $\sim(\nu^3/\varepsilon)^{1/4} < 1 \cdot 10^{-3}$ m. The dissipation rate of turbulent kinetic energy is equal to the supply rate fed by the vortex motions of

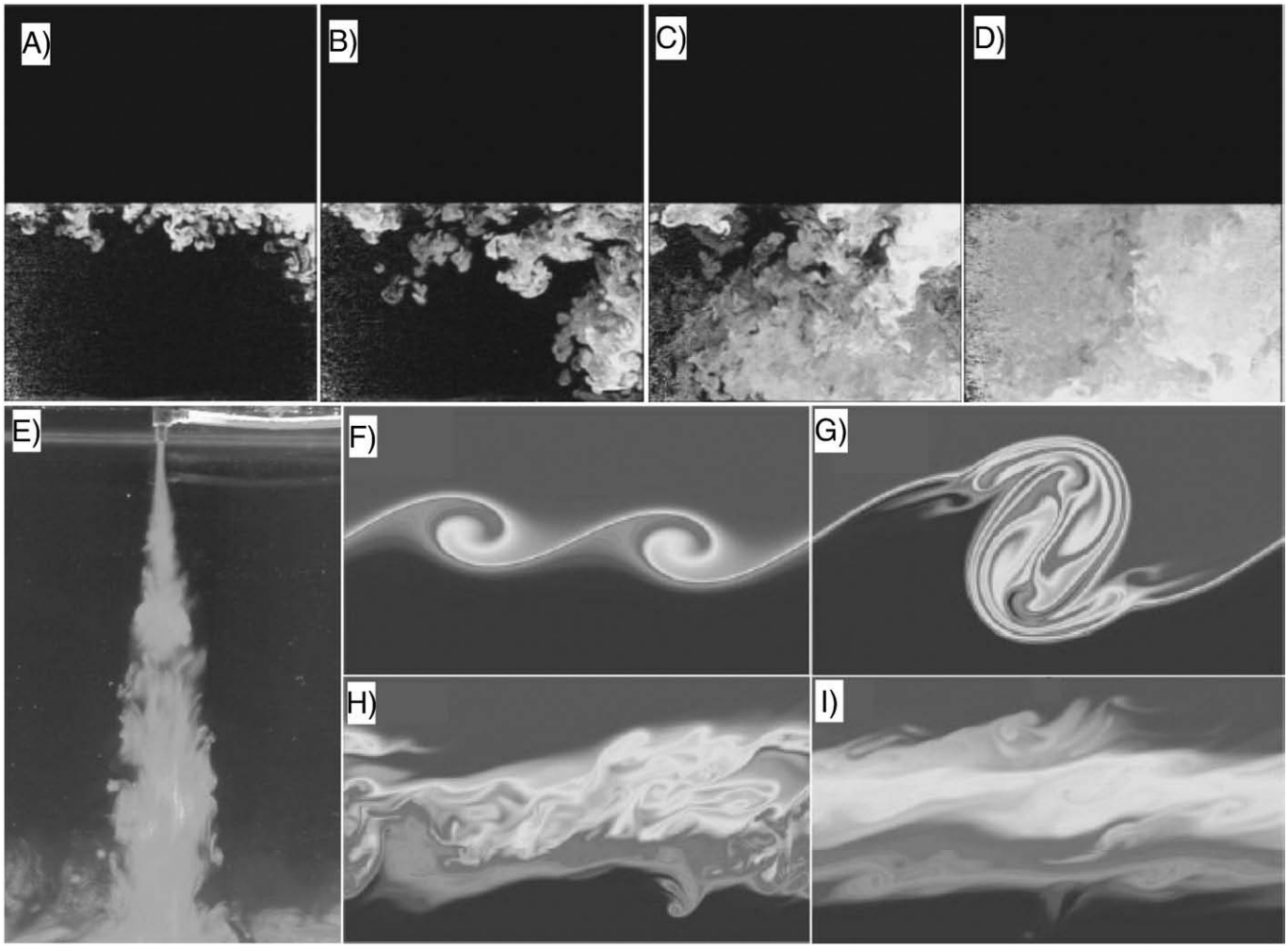

Fig. 1. A schematic overview of hydrodynamic instabilities leading to turbulent mixing. In panel A–D the evolution of RT instability is shown in natural photos using Light-Induced Fluorescence. The upper half of the container is blocked and black (Dalziel et al., 1999). In panel E shear instability on vertical walls drives horizontal entrainment of material into a buoyant jet. The width of the entrainment zone increases linearly with depth. In panels F–I, the classical KH-instability is illustrated, where turbulent mixing occurs by roll-up of KH-billows in horizontal flow (Smyth et al., 2001).

the largest eddies, at $\varepsilon \sim U_c^2/(L/U_c) = U_c^3/L \approx 10^3\ \mathrm{m^2\ s^{-3}}$ (Tennekes, 1972), where $L \sim 1000$ km and $U_c > 0.1$ km/s, are the characteristic dimension and (post-impact) speed of the largest eddies, respectively. Note the Kolmogorov micro scale is little sensitive to ε. Thus, being wrong by a factor of 100 only changes the length scale by a factor of 3! Importantly, turbulent vortex shedding proceeds down to sub-centimeter scale at which elements diffuse in a few hours.

We expect that the analysis by (Dalziel et al., 1999) is applicable to our problem since the consequences of the primary difference (immiscibility in our case, miscibility in their case) are not encountered except at the smallest scales. The fact that we are dealing with much larger density differences should not matter since the scaling with respect to that parameter is taken fully into account.

For a system initially at rest, the thickness of the mixing zone, h, grows quadratic in time from an unstable boundary (Dalziel et al., 1999):

$$h^* = \alpha^* A g t^2 \tag{2.1}$$

Here, g is gravity, $A = (\rho_2 - \rho_1)/(\rho_1 + \rho_2)$ is the Atwood number and ρ's are densities "1" and "2" refers to (lower) silicate and (upper) iron, respectively. The constant α^* is determined empirically and has to do with the turbulent motions. Several authors find the value to be ~0.06 for rising fluid, formally known as bubbles, and ~0.07 for sinking fluid known as spikes (Dalziel et al., 1999). In all of our analysis, we will use $\alpha = 0.06 + 0.07 = 0.13$ and reserve h for the entire mixing zone (bubbles and spikes). Experiments show that Eq. (2.1) remains valid even though the exponential growth of larger length scale RT instabilities is present as time progresses. One way to see why this might be true is to note that the inverse of the characteristic timescale for a linear instability (i.e., exponential growth) with wavelength h (the thickness of the mixed zone) approximately satisfies Eq. (2.1) in the inviscid limit (as indeed it must by purely dimensional considerations, there being no other parameters of relevance). Thus, quadratic growth persists even though there are exponentially growing instabilities at ever-longer wavelengths.

To clarify this physical picture, consider the following (unrealistic) scenario. Suppose a 1000 km thick layer of liquid iron is at rest on top of a terrestrial magma ocean of even greater thickness. Ignore spherical geometry and variation of g with depth. Complete emulsification will be achieved once the mixing layer reaches $h \sim 2000$ km (i.e., it has propagated to the top of the iron layer as well as downwards by ~1000 km). This will be achieved in a time frame of $t = (h/\alpha A g)^{1/2}$ ~2000 s or only 5 times longer than the free-fall time through 2000 km!

The driving force for RT-instability is the pressure gradient difference across the boundary and can be represented by an effective gravity, g_{eff}, where the z-axis is positive along target gravity g_0.

$$g_{\mathrm{eff}} = [(dp/dz)_2 - (dp/dz)_1] / (\rho_1 + \rho_2) \tag{2.2}$$

In the above example the effective gravity is given by $g_{\mathrm{eff}} = A g_0$. We shall keep in mind that there is a simple relationship between effective gravity and pressure gradient differences across the RT-unstable boundary, and turbulent mixing arise when $g_{\mathrm{eff}} > 0$.

2.2. Rayleigh Taylor erosion models

During a giant impact the iron starts out in motion relative to surrounding silicates and this significantly changes the degree of emulsification by Rayleigh–Taylor instability. Insights into restoring forces that stabilize the iron–silicate boundary are illustrated in the following model, in which a sphere falls through a silicate magma ocean.

2.2.1. RT-erosion from a sinking core at constant velocity in a constant gravity field

Suppose a sphere of metal with radius R falls vertically through a silicate magma ocean at speed U (Fig. 2A). Erosion of metal can occur from the lower boundary of the sinking sphere (the upstream part of the flow). Let's first assume that the acceleration due to gravity is completely balanced by the drag forces on the sphere (the sphere is sinking at terminal velocity). Since neither the silicate nor the metal is accelerating, the fluid pressures are hydrostatic on either side of the interface, except for the centrifugal effect associated with the flow around the sphere. As the core penetrates downward the mixing zone below the sphere grows quadratic in time (Eq. (2.1)) and transient silicate erodes iron from the core. The flow of silicate around the sphere is assumed to be steady and incompressible.

Consider the frame of reference where the sphere is at rest and the silicate flows around the obstacle (Fig. 2A). In reality there is a shear layer adjacent to the silicate-iron interface. The liquid iron has low viscosity and will flow upwards relative to the center of the sphere), tending to match the silicate velocity. The flow within the iron sphere is accordingly a closed circulation, upwards at the periphery and downwards near the center. It is nonetheless possible that the shear influences the development of the RT instability. We appeal here to laboratory experiments (Snider and Andrews, 1994), which suggest that this is not a major effect on the quadratic growth of the mixed layer. Our picture of what happens is obviously most correct near the basal (more nearly horizontal) part of the silicate–liquid interface and becomes increasingly inaccurate as one approaches 45 to 90 degree angles away from the horizontal. One must there expect the large-scale KH instabilities to have some effect.

The fluid passing by the sphere follows (on average) a path with angular coordinate $\theta = Ut/R$. The growth rate of the mixing zone (Eq. (2.1)) is:

$$dh/dt = 2\alpha A g(\theta) t \tag{2.3}$$

The mixing zone (Fig. 2A) is approximated by a cylindrical symmetric region below the sphere of height $h(\theta)$ and width $R \cdot \sin(\theta_{\max})$ and mean silicate particle speed U.

The mixing rate is:

$$dV_{\mathrm{mix}}/dt \approx 2\pi R \sin(\theta_{\max}) U h_{\max} \tag{2.4}$$

where

$$h_{\max} = \int 2\alpha A g(\theta) t dt \tag{2.5}$$

Eq. (2.5) represents the maximal height of the mixing zone as iron sweeps around the sphere. This is found by integration over the time period a silicate particle travels inside the mixing zone:

$$h_{\max} = 2\alpha A (R/U)^2 \int_0^{\theta\,\max} g(\theta)\theta d\theta \tag{2.6}$$

$\theta_{\max}$ sets the range of the RT-unstable zone, thus $g(\theta_{\max}) = 0$. In this way the mixing fluids are swept behind the core.

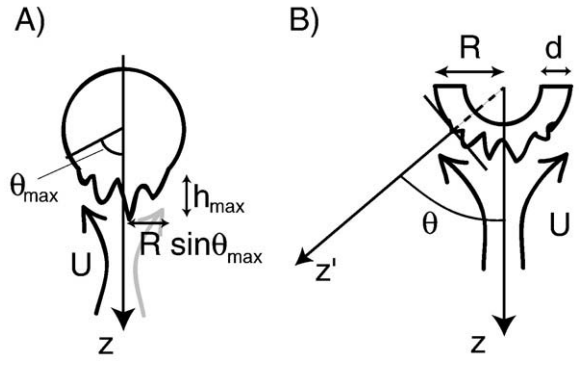

Fig. 2. Geometrical parameters used in the RT-erosion models: A) spherical core B) hemispherical sheet. The mixing zone is cylindrical symmetric about the z-axis, with radius and height given by $R\ \sin\theta_{\max}$ and $h_{\max}$, respectively. The hemispherical sheet has radius, R, and thickness, d.

We define efficiency of emulsification by the ratio of the mixed iron to initial volume of metal core and assume the mixing zone contains even mixture of silicate and metal, Eff $= V_{mix}/2V_0$ with $V_0 = 4\pi R^3/3$. The distance traveled is measured in units of magma ocean depth, H, by substituting $dx = U dt/H$, and the efficiency estimate yields:

$$d(Eff)/dx = \beta\alpha A g_0 H / U^2$$
$$\text{with } \beta = 3/2 \sin(\theta_{max}) \left[\int_0^{\theta max} g(\theta)\theta d\theta / g_0 \right]. \quad (2.7)$$

In this simplistic model, effective gravity is constant and the vertical part of the gravity vector is $g(\theta) = g_0 \cos\theta$, so that the width of the unstable zone is $\theta_{max} = \pi/2$ and $\beta = 3/2(\pi/2 - 1) \approx 0.86$. Substituting values from SM-Table A1 yields Eff ~ 0.032 gH/U^2. Cores descending at $U = 1$ km/s are completely emulsified cores (Eff = 1) after penetrating ~3125 km into the silicate magma ocean. This illustrates how efficient mixing requires the involvement of a significant portion of Earth's mantle (2890 km). We investigate the more realistic model where the pressure gradient difference across the silicate–metal boundary also includes local gravity field and fluid flow around the sphere.

2.2.2. Generalized RT-erosion from a sinking core

The driving force of RT-instability changes as the impactor's core sinks through the mantle and when self-gravity on the largest cores modifies the local gravity field. Analytical solutions have been derived for effective gravity and flow speed as a function of depth, and Eff is calculated by same means as in the example above. Details are stored in Supplementary Material A. This model assumes that the metal blob remains spherical and coherent during the descent through liquid silicate. In reality, the core is liquid and will deform, and we have investigated how shape matters for the mixing efficiency by applying the same analysis for hemispherical sheets (Fig. 2B). This means emulsification depends also on *flattening* defined as the aspect ratio R/d, where $R/d = 1$ is equivalent to a half sphere. A half sphere emulsifies roughly twice as fast as a full sphere (Figs. 3 and 4) with a small difference appearing from changes in flow speed. *Eff* becomes a function of size (R or equivalent sphere radius R_{eqv}), shape (aspect ratio R/d), magma ocean depth (H), and initial flow speed (U_0). Due to imperfect knowledge about other physical parameters in the model (i.e. turbulent drag coefficient, c_D), the uncertainty of Eff is estimated to a factor of 2.

Complete emulsification down to centimeter scale occurs for spherical iron cores with initial radii smaller than 1–4 km (Figs. 3A and 4A), equivalent to terrestrial planetesimals with a radius of 1.6–6.5 km. The critical core size is insignificantly modified by changes in the initial speed of post-impact flow between 0.1 km/s and 10 km/s. For giant impacts, the entire iron core does not emulsify. Only 0.7 wt.% of an iron core with 1000 km radius mixes by RT erosion in a vertical fall through a maximal magma ocean, 3000 km deep. Clearly, large cores have big influence on siderophile depletion in silicate Earth, since mixing ~0.7 wt.% of a 1000 km core is equivalent to mixing 100 wt.% of a 190 km core; however, massive iron cores >4 km plunge into the Earth's core and do not share their chemical constituents with the mantle. Consequently, most of the Earth's core did not equilibrate with silicate during the later stages of planet accretion (we return to a derivation in Section 3).

Efficiency of emulsification increases for thin cores where the thickness of metal is much reduced (Fig. 3B). This is illustrated in Fig. 4B, where a 32 km core (equivalent sphere radius) completely erodes if it spreads into sheet with aspect ratio 1:7, corresponding to a 1 km thick iron sheet. A factor of 2 uncertainty of the efficiency estimate propagates roughly linearly to critical core radius in both cases with spherical and hemispherical sheets (Fig. 4A). Conclusively, the physical picture is clear: 1) very large cores do not equilibrate efficiently 2) flatter cores mix faster 3) slow start (low U_0) enables emulsification of insignificantly larger cores.

Most impacts are inclined relative to target gravity ($\Theta \sim 45°$) so that sinking cores travel along non-vertical trajectories. This would change the efficiency of RT-erosion in a number of ways. Simple scaling Eff ~ g_{eff} (θ_{max}) H/U^2 suggest an increase of $1/\cos(\Theta) \sim 40\%$ due to longer trajectory. Counteracting this, the driving force for RT instability is reduced by a centrifugal force that acts along the radius of curvature of the trajectory (perpendicular to its velocity) adding a component opposing target gravity. The centrifugal acceleration is of order $a_{cen} \sim (U \sin\Theta)^2/R \sim gR\sin^2\Theta/R \sim g \sin^2\Theta$ and will typically reduce effective gravity by ~30% when the core is sinking at terminal velocity $U \sim (gR)^{1/2}$. Hence, our main conclusion that large cores do not emulsify entirely in the vertical impact scenario also holds in the non-vertical case.

Possible explanations for faster or additional equilibration include: 1) Small cores mix at higher rate because the radius remains fixed in our efficiency integration and hence overestimates the stability of the core. This is, however, a small correction on the largest cores. 2) Additional erosion may take place on the backside of the core by highly turbulent wake flow. 3) Iron droplets may equilibrate with a

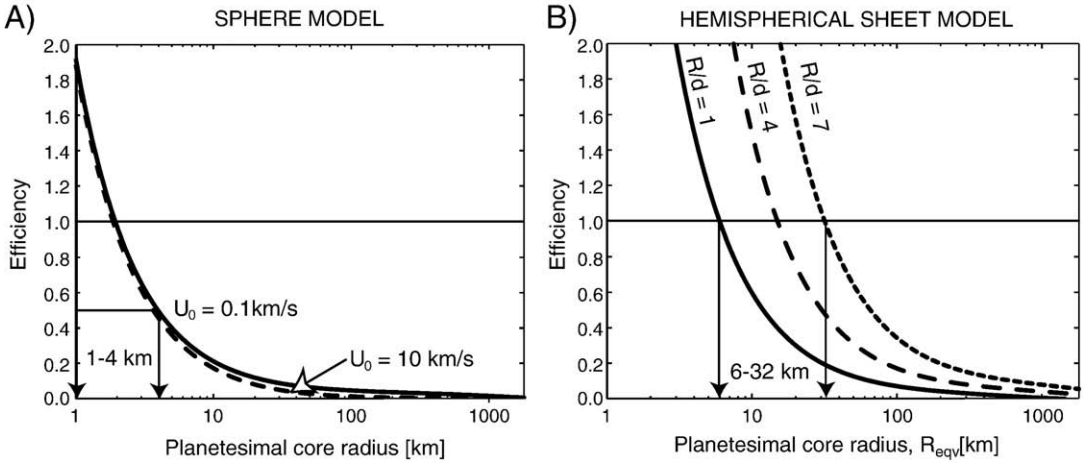

Fig. 3. RT erosion model: Efficiency of mixing versus metal core radius (semi-logarithmic axis) for A) spheres and B) hemispherical sheets. The solid and dashed curves in A) represent scenarios with initial speed $U_0 = 0.1$ km/s and 10 km/s, respectively. Complete emulsification is illustrated by the thin line Eff = 1. The efficiency estimate carries a factor of 2 uncertainty leading to critical iron core radius of 1–4 km. The curves in B) show efficiency of emulsification for a hemispherical sheet at an initial vertical velocity of $U_0 = 1$ km/s for various aspect ratios: $R/d = 1$ (solid), $R/d = 4$ (dashed), and $R/d = 7$ (dotted). The thin line illustrates complete emulsification. It is clear that flattened cores mix more efficiently. The model uncertainty propagates approximately linearly between efficiency and critical core size, so that an iron cores with 16–64 km radius can mix if spreading into a sheet with aspect ratio $R/d = 7$.

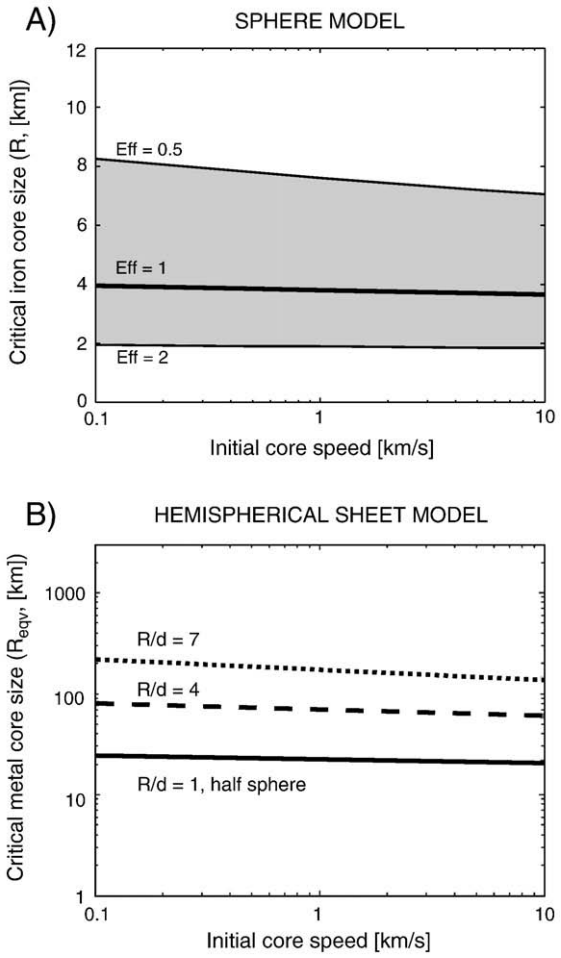

Fig. 4. A) Critical core size versus initial core speed (semi-logarithmic). Planetesimal of 2–7 km radius (with core radius 1–4 km) emulsifies completely inside a 3000 km deep magma ocean. The efficiency estimate carries a factor of ~2 uncertainty (grey region) for any reasonable values of initial flow speed. B) The critical size for hemispherical sheets versus initial flow speed U_0 is shown for various aspect ratios, $R/d=1$ (solid), $R/d=4$ (dashed), $R/d=7$ (dotted). Notice the logarithimic y-axis.

much larger reservoir of silicate in the posterior flow after the core has sunk through the mantle. 4) Mixing by shear instability adds to the emulsification process by creating sheets and distortions that increase surface area available to RT.

In numerical simulations of the lunar forming impact (Canup, 2004) highly distorted iron cores of long, thin shapes appears during the impact scenario, and we evaluate the possibility that the majority of mixing occurs by shear instability on vertically thin structures.

2.3. Shear-driven instability and turbulent structure

In the classical Kelvin–Helmholtz (KH) instability fluids of different density mix by shear forces and gravity acts as a restoring force (Fig. 1 F–I). A disturbance of the interface between liquid iron and silicate will grow in amplitude if its wave length is sufficiently small $<430\ \mathrm{km}\cdot(\Delta U/1\ \mathrm{km/s})^2$ (Chandrasekhar, 1961c). Here, ΔU is the tangential velocity difference of the two fluids. Shear forces roll up dense material into spiraling structures, known as KH-billows, to a maximal overturn scale height characterized by the Thorpe scale $L_T=\Delta U^2/(2Ag)\sim 150$ km (Smyth and Moum, 2000). The fluids inside a KH-billow stretch into thin layers and may cause intimate mixing down to a small scale where isotopes equilibrate even for the largest billows.

In the case of vertical shear instability, gravity does not act as a restoring force, and the mixing zone will expand faster. Therefore, shear driven mixing is probably prominent across vertical walls. In numerical models (Canup, 2004), the metal core of the impacting body is stretched into a long cylindrical projectile prior to impact which, then, penetrates vertically through the silicate mantle. Ambient fluid will entrain by vortex motions into the deep interior of the metallic core (Fig. 5) and the width of the cylinder will expand linearly with depth into a cone-shaped structure as the bulk iron core proceeds downwards (Morton et al., 1956).

The dynamics of the stream and expansion of the entrainment zone will change from jet-like to plume-like in the uppermost 100–500 km of the mantle, when the flow changes from momentum-driven to buoyancy-driven. This is known to occur at a distance of 1–5 times the Morton length scale $l_M=(M)^{3/4}/B^{1/2}\sim 100$ km $(U/1\ \mathrm{km/s})(D/100\ \mathrm{km})^{1/2}$ characterizing the relative importance of momentum fluxes $M=QU$ and buoyancy fluxes $B=g(\Delta\rho/\rho_m)\,Q$ in cylindrical jets (Papanicolaou and List, 1988). Q and U are the initial volume flux and the velocity of the jet/plume, respectively. In a deep magma ocean metal cores would expand mostly in a plume-like fashion with the width of the entrainment zone h increasing linearly as a function of travel distance, z: $dh/dz=\alpha_{plume}\approx 0.1$. This value is higher for plumes than for jets $\alpha_{jet}\approx 0.05$ (Turner, 1986).

An estimate of 'mixing' can be defined as the situation when the entrainment zone contains 50% impactor metal and 50% ambient silicate from target and impactor. The geometrical constraint for mixing cylindrical cores of height, h, and diameter, d, is $V_{mix}=2V_{core}=2\pi L(d/2)^2$, where V_{mix} is the conical volume with cut-off tip of height, small and large diameter are L, αH, $\alpha(H+L)$, respectively. The mixing efficiency is overestimated by ignoring the slow expansion in the jet-like regime. Horizontal entrainment by shear instability is mixing impactors up to ~450 km equivalent sphere radius (Fig. 6). The expansion of the mixing zone is fastest for thin cylindrical impactors, with aspect ratio $L/d=7$, where the entrainment proceeds in plume-like fashion ($\alpha_{plume}\approx 0.1$), and the magma ocean is deepest, $H=2500$ km. Larger bodies would need to disrupt prior to the sinking through Earth's mantle. This estimate for mixing is very conservative, because a large fraction of the mixed silicate might come from the impactor itself leaving the majority of the target mantle unmixed with the impacting core. More importantly, mixing on large scales does not guarantee equilibration of isotopes. We need to understand if turbulent motions disrupt metal and silicate into centimeter scale where diffusion is fast and isotopes can equilibrate.

The latter seems problematic for vertical shear instability. Turbulent motions in the entrainment zone are fed by large-scale vortices of length comparable to the width of the jet/plume b_w. Naively, one would expect a

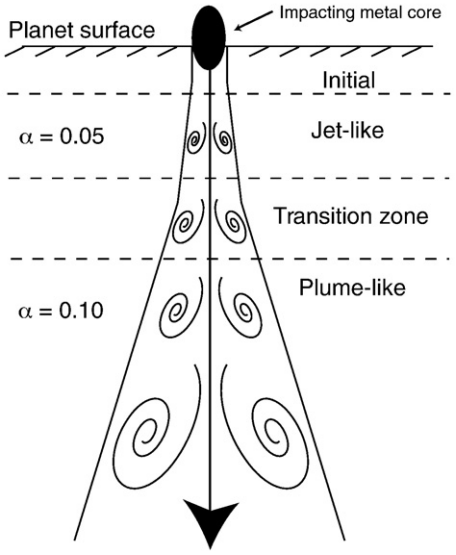

Fig. 5. Shear instability on vertical walls for a cylindrical jet/plume of metal. Ambient fluid is entrained into the metallic cylinder causing the mixing zone to expand linearly with depth. The expansion begins at a depth comparable to the diameter of the cylinder, in a momentum-driven (= "jet-like") manner. As the flow becomes buoyancy-driven ("plume-like") the width of the entrainment zone will expand at a faster rate.

Kolmogorov cascade in RT-sense, in which turbulent energy is rapidly transferred into smaller and smaller eddies. This appears to be true at the small length scales, but apparently there is a characteristic scale k_b^{-1} above which buoyancy forces appreciably modify the energy spectrum and eddy shedding from larger to smaller scales is slow. This conclusions is based on experimental studies by Kotsovinos (1990) justified by theory (Okamoto, 1996). Both suggest a -3 power law turbulent energy spectrum when the characteristic wave number $k=2\pi/\lambda$ is in the range $k_c<k<k_b$. The largest cores represent the scale, k_c, and the smallest is given by $k_b=\Phi_O^{3/4}\varepsilon^{-1/2}$ where Φ_O and ε is the gradient of the mean buoyant force and turbulent dissipation rate, respectively. There is a fundamental difference between the two energy spectra. A -3 power law has much less energy at the smallest scales compared to a Kolmogorov spectrum. Since energy is fed from the largest eddies, the -3 power law resemble turbulent flow where eddy shedding is relatively slow. Most of the iron does not mix below k_b^{-1} (kilometer size, Supplementary Material B) and never mix at centimeter scale where equilibration can occur.

Even though the entrainment zone is not intimately mixed at the centimeter scale, large eddies still possess considerable amounts of energy, which eventually dissipates into heat or surface energy (droplet formation) at $<10^{-3}$ m length scales. Therefore, it is still possible that the bulk iron and silicate can mix on length scales smaller than ~kilometers in the post-impact aftermath.

In addition to these uncertainties, there exist a range of modifications to the models presented here. Some unstudied effects include density stratification in the mantle and the dynamics of rotation (e.g. the Coriolis force).

3. From core formation mixing models to Hf–W evolution

The fraction of Earth's core that equilibrated during core formation, Φ_m, can be estimated from the efficiency of emulsification, Eff, if the mass distribution $\phi(m)$ of accreting bodies is known.

$$\Phi_m = \int_{\text{all } m}(\text{Eff}\cdot m)\phi(m)dm \tag{3.1}$$

Here $\phi(m)=\mathrm{d}n/\mathrm{d}m$ where n is the number of planetesimals with mass$<m$. Φ_m is evaluated by adopting a mass distribution of accreting bodies given by a power law: $\phi=A_m m^{-\eta}$ with a normalization constant determined so that the core is fully equilibrated $\Phi_m=1$, when all accreting cores complete emulsify, Eff $=1$. That is $\int_{\text{all } m}\phi(m)$ $m\,\mathrm{d}m=M_{\text{Earth}}$. These bodies are conveniently chosen at masses ranging from zero (e.g. dust) and to the Moon forming impactor at 0.1 M_{Earth} (Canup, 2004). In reality the distribution of impacting bodies may not form a power law and may instead be split into two classes of bodies, the runaway embryos (lunar mass to Mars mass) and the small planetesimals that are needed to provide the dynamical friction inferred from the observed eccentricities and inclinations of the terrestrial planets (O'Brien et al., 2006). However the use of a power law will serve as an illustrative example. The range of size-frequency distributions used for the present main asteroid belt and Near Earth Objects have $\eta=1.65$–1.83 (Ivanov et al., 2002). The slope of the power law characterizes how many small bodies accrete; for example $\eta=1.65, 1.74, 1.83$ corresponds to 55%, 45%, and 32% of Earth's mass accreting as bodies with >1 wt.% of Earth's mass (radius >1370 km).[1] Values closer to 2 result if planetesimals disrupt into smaller bodies prior to impact. Our analysis yields Φ_m between 0.1–25% and many solutions around 10% ($\eta=1.65$–1.83 and $R/d<7$) (Fig. 7). Near efficient equilibration can occur only if cores disrupt into smaller bodies prior to impact.

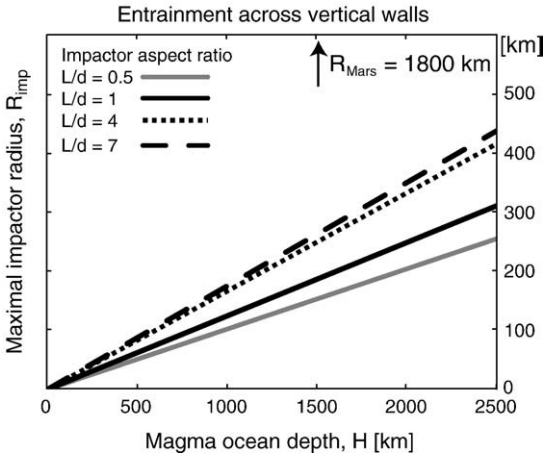

Fig. 6. Entrainment across vertical walls for a cylindrical plume of length, L, and diameter, d, allows mixing of metal and silicate. The maximal size of impactors at which the mixing zone contains 50% metal from the impactor and 50% silicate from impactor + mantle is shown as a function of magma ocean depth for various impactor aspect ratios, L/d. This model overestimates equilibration of isotopes since mixing may occur only at the largest scales where diffusion and isotopic equilibration is slow (see Section 2.3 for details), yet the largest cores are unable to mix metal with surrounding silicate even on the largest scales. Impactor radius is given as equivalent sphere radius, R_{eqv}.

Even in the case where $\Phi_m=1$ and the Earth's core completely equilibrated with the silicate mantle, complete equilibration of the silicate Earth cannot be guaranteed. For example, the Earth's mantle is twice as massive as the core, which principally means 1 kg metal is responsible for the equilibration of 2 kg silicate. In our RT erosion models iron and silicate mixes in equal volumes and because of the density ratio of iron to silicate is ~2, maximally one fourth of the silicate mass can be processed through the RT-mixing zone. The rest would depend on what happens in the posterior flow. Therefore, we distinguish between Φ_m and Φ_s that defines cumulative fractions of the metallic core and silicate mantle that equilibrated during core formation, respectively.

The two parameters Φ_m and Φ_s are related. If all iron cores were to break down rapidly to centimeter size droplets upon impact or within the uppermost few kilometers, each droplet could deplete the entire cylindrical column of siderophile elements on its way through the magma ocean. The minimum mass of metal, $m_{\text{metal,min}}$, needed to deplete the mantle inventory of W occurs in deep magma ocean of mass m_{silicate} and require the partition coefficient, efficiency of mixing and metal/silicate inventories of certain sizes: $K_W\cdot \text{Eff}_m\cdot m_{\text{metal,min}}/m_{\text{silicate}}\sim 1$, where K_W is the partition coefficient for W into the metal phase, e.g. $K_W=[W]_{\text{metal}}/[W]_{\text{silicate}}$ (ratio of moles/kg) in the two phases after the metal–silicate mixture has equilibrated and separated. Siderophile elements in the mantle are scavenged into the core, if K_W and Eff_m are sufficiently large. Specifically, the cumulated metal–silicate equilibration must exceed $\Phi_m>1/K_W$ for the mantle W to "see" accreting core metal. As emulsification is slow and limits metal–silicate equilibration ($\Phi_m\ll 1$), the silicate Earth is unable to share its siderophile elements with the core. The estimated W partition coefficient during the last major metal–silicate equilibration event is ~16 (Righter et al., 1997; Drake and Righter, 2002; McDonough, 2003). At this value, our results ($\Phi_m\sim 0.1$) suggest that complete equilibration of the silicate mantle is not guaranteed when the iron and silicate are liquid. Clearly, a single giant impact has limited capacity to reset the ^{182}W excess in the mantle.

3.1. Hf–W chronometer

Initial interpretations of the Hf–W chronometer suggested an early formation of the Moon (<50 Myrs) based on the excess $\varepsilon_W=1.9$ in bulk silicate Earth relative to chondrites (Kleine et al., 2002; Yin et al., 2002). This assumes the Earth to have formed from a chondritic reservoir and that siderophile isotopes and elements fully equilibrated between metal and silicate during all stages of core formation. Recently, the lunar and terrestrial mantles were found to have identical ε_W (Touboul et al., 2007), which provides strong evidence that the Moon-forming impact and the final stages of Earth's core formation took place after the extinction of

[1] The fraction of the Earth which arrives in chunks larger than m_0 is then $F_0=1-(m_0/m_{\max})^{2-\eta}$.

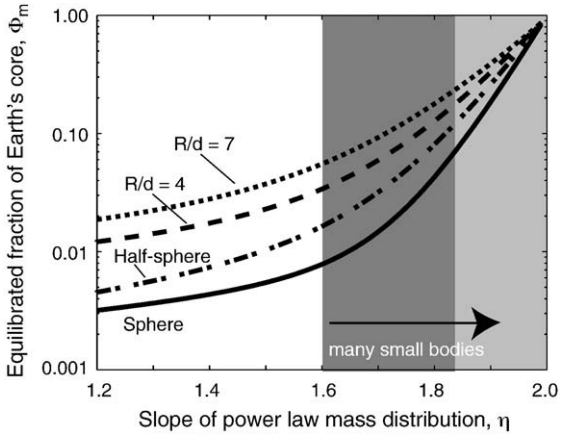

Fig. 7. Cumulated fraction of Earth's core that equilibrated with silicate during core formation (Φ_m, semilogarithmic axis) versus slope of the mass distribution power law, η, according to efficiency estimates from our RT-erosion models. The curves represent various geometries of sinking cores: sphere (solid), half sphere (dot-dashed), and hemispherical sheets with $R/d=4$ (dashed) and $R/d=7$ (dotted). The Earth's core accretes with incomplete metal equilibration with the silicate mantle for accretion histories dominated by large cores (small η values), simply because the largest metal cores are unable to emulsify down to length scales where equilibration can occur. Preferred values for η are shown in the dark grey region. For small η, the half sphere model predicts too high core equilibration, Φ_m, because self-gravity has been overestimated. However, a correction is only necessary outside the shaded region.

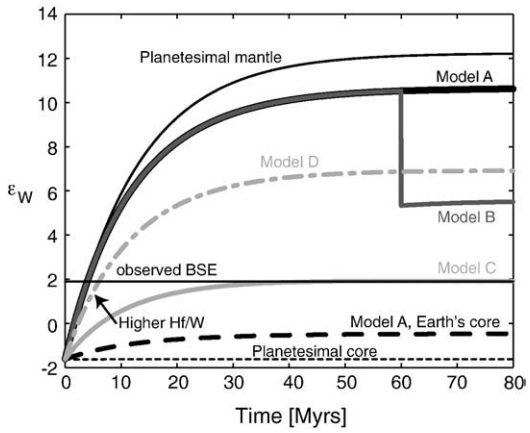

Fig. 8. Time evolution of ε_W for various models of continuous core formation. Mass accumulates at an exponentially decreasing rate, such that 63% of the Earth has accreted after 11 Myrs (Yin et al., 2002). The range of accessible values is enveloped by the early-formed mantles (uppermost thin black curve, $\varepsilon_W=12$) and early-formed cores (lowermost dashed curve, $\varepsilon_W=-1.9$). Hf/W fractionation in the silicate reservoirs causes a steeper slope. In model A (mantle = thick solid black curve, Earth's core = thick dashed black curve) the Earth accretes without equilibrating metal from the accreting cores, but the silicate mantle of the impactors does equilibrate with their cores prior to impact, so that silicate Earth is diluted relative to the scenario when the mantle is fractionated at an early stage and left untouched ever after. Model B is similar to model A except that 10% of the Earth's mass accretes at 60 Myrs with unrealistically high degree of equilibration: all metal completely equilibrates with the entire silicate mantle. Notice that the giant impact does not reset the mantle to the chondritic value. The effect of constantly incomplete equilibration, for example a hidden silicate reservoir, is shown in model C (solid light grey curve) and model D (dot-dashed light grey curve) where the equilibrating fraction of silicate Earth is 53% and 10%, respectively.

^{182}Hf (i.e. >50 Myrs) (Kleine et al., 2009). Thus, the initial assumptions were apparently wrong in stating that the ε_w excess relative to chondrites could be linked to early core formation. What, then, is the significance of ε_w enrichment in bulk silicate Earth, and will it tell us about the style of core formation?

A schematic overview of ε_W evolution in the silicate Earth is shown in Fig. 8 for a variety of core formation scenarios. In all cases silicate Earth and chondrites gain radiogenic W at an exponentially decreasing rate, $\varepsilon_W \sim (1-e^{-\lambda t})$. In the simplest case (model A) the current Hf/W ratio in the mantle is achieved very early and the silicate did not experience further equilibration (e.g. $\Phi_s=0$). This case has a particular simple analytical solution (derivation in Supplementary Material C):

$$\varepsilon_W = \left(1 + f_{met/sil} K_W^{mean}\right)\left(^{182}Hf/^{182}W\right)_{BSSI} \cdot 10^4 \quad (3.2)$$

$$= \left(1 + 0.47 \cdot 16\right) \cdot 1.39 \cdot 10^{-4} \cdot 10^4 = 12$$

A similar high value of $\varepsilon_W \sim 18$ is derived by continuous core formation models when metal–silicate is set not to equilibrate and the last major metal–silicate equilibration occurred early in the accretion history (Kleine et al., 2005b).

Late equilibration ($\Phi_s>0$) changes the ε_W evolution both by changing the Hf/W ratio in the mantle (arrow in Fig. 8) and by resetting ε_W to the chondritic value. The first aspect is mainly controlled by how the partition coefficient changes over time (temperature, pressure, oxygen fugacity). The second issue needs further considerations. Suppose the impactor has chondritic composition. The radiogenic mantle will be diluted instantaneously at the impact, if either the impactor equilibrated immediately before impact or if all radiogenic W from the impactor's mantle and all unradiogenic W from its metal core were involved in post impact equilibration. This

Table 1
The predicted effect on ε_W in bulk silicate Earth for various impact driven accretion scenarios. The values shown represent the offset from a reference model, where $\varepsilon_W=1.9$ is obtained using a non-truncated, continuous mass accretion, $dM/dt=\lambda \cdot M_{Earth} \cdot e^{-\lambda t}$ with a characteristic time scale $\tau_{acc}=\ln(2)\cdot\lambda^{-1}=4.7$ Myrs (similar to model A in Fig. 8). The mass of the impactor is 0.1 M_{Earth} and the W partition coefficient is kept constant, at $D_w=16$, corresponding to W concentrations in core and mantle of 262 ppb and 16 ppb, respectively. The effects are enhanced by a factor of <2 using a two-fold higher partition coefficient, $D_w=32$. In any case, the timing of last giant impact is one among several parameters of equal importance.

Time of last GI (Myrs)	Full equilibration	Hidden reservoir effect		Core crash[c]		Combined
		Far side[a]	Far side + deep mantle[b]	Major 98 (%)	Minor 50 (%)	Far side + major core crash
The impactor last equilibrated at t = 0						
30	−0.6	−0.4	−0.3	+0.9	−0.0	+0.9
60	−0.9	−0.7	−0.5	+1.0	−0.2	+1.0
120	−0.9	−0.7	−0.5	+1.0	−0.2	+1.0
The impactor equilibrated immediately before the impact						
30	−0.6	−0.4	−0.3	−0.1	−0.4	−0.1
60	−0.9	−0.7	−0.5	−0.2	−0.6	−0.2
120	−0.9	−0.7	−0.5	−0.2	−0.7	−0.2

Causal effect on ε_W in parts per 10,000 in bulk silicate Earth for various accretion scenarios with a late Moon forming impact.
[a] Far side = 50% of silicate Earth is not equilibrating during the giant impact.
[b] Deep mantle = Further 50% of silicate Earth (total 75%) is hidden and do not equilibrate during the giant impact.
[c] Core crash = A fraction of the impactor's metal core do not equilibrate during the giant impact.

extreme case means that the core formation history of the projectile is lost. This kind of scenario has been suggested where the lunar forming impact alone is responsible for resetting silicate Earth from $\varepsilon_W \sim 10$ to 1.9 (Kleine et al., 2004). Model B in Fig. 8 shows an example of this unrealistic scenario. Our fluid dynamical models contradict such a scenario, simply because the ratio of W arriving by the giant impact to W residing in the mantle of Proto-Earth is not substantially larger than unity.

Moreover, it is hard to imagine efficient resetting by the last major impact without having somewhat similar degree of resetting at the previous giant impact events (10–60 Myrs), because the degree of equilibration during a Moon forming impact with a mass of 0.1 M_p is not substantially different from an impact with a 0.05 M_p or even 0.01 M_p object. Therefore, the modest ^{182}W enrichments are most easily explained if ε_W never dramatically exceeded ~1.

The silicate Earth obtains the ε_W value given by the mixture of non-equilibrating mantle and the mixture of equilibrating metal and silicate (from both bodies). At low metal equilibration efficiency, accreting metal cores plunging through the mantle deliver metal to the target core, rich in W with a depleted ε_W signal. The remaining, equilibrating fraction of the impactor would therefore have super-chondritic composition and the silicate Earth would no longer reset to the chondritic value ($\varepsilon_W = 0$). This case is illustrated as model C in Fig. 8 where core formation proceeds continuously with a constant metal equilibration Eff = 53% at all stages of core formation using a characteristic accretionary time scale $\tau_{acc} = 11$ Myr. Incomplete equilibration leads to higher ε_W. This is illustrated in model D in Fig. 8 with a constant metal equilibration, Eff = 10%.

3.2. The last giant impact

The ability to reset mantle ε_W by one single impact is determined by $A = K_W \cdot \mathrm{Eff} \cdot m_{impactor}/m_{target}$. As $K_W \cdot m_{impactor}/m_{target}$ is of order unity only and a large fraction of the impactor's core ($1\text{-}\mathrm{Eff}_{GI}$) may crash directly into Earth's core, one single large impactor has limited ability to set mantle ε_W. If the partition coefficient and the efficiency of equilibration were larger, a single impactor could have a big effect on the Hf–W chronometer. Moreover, temperatures during a giant impact may be super-critical as indicated in SPH simulations (Canup, 2004) at which the partition coefficient must be of order unity, and siderophile/lithosphile budgets in the mantle are left unchanged.

The consequence of a single giant impact on ε_W is rather small no matter when it happened (Table 1). For example, a giant impact occurring at 60 Myrs will reduce ε_W by one unit if the entire impactor equilibrates with the Earth's mantle. However, this signature depends on how much of the silicate and iron participates in equilibration. For example, there would be a *hidden reservoir effect* of silicate not seen by the impactor, e.g. the far side of the planet and, perhaps, the lower part of the mantle, which might have been frozen and therefore would not have equilibrated chemically with the rest of the mantle (Sasaki and Abe, 2007; Golabek et al., 2008). Also, the fraction of the impactor's metal plunges directly through the Earth's mantle into the core, denoted as the *core crash effect*. The major changes to ε_W in bulk silicate Earth is controlled during early core formation when Hf/W fractionation was first established, with the last giant impact capable of only slight modification of a magnitude similar to the uncertainty caused by hidden reservoir and core crash effects.

4. Implications

The final stages of Earth's accretion (10–100 Myrs) occurred by large impacts of differentiated objects, which means core formation occurred between massive iron bodies in an impact-driven manner. Rayleigh–Taylor instability leads to fast turbulent mixing and eddy shedding down to length scales where tungsten (and other siderophiles) can equilibrate. However, our models suggest large cores >10 km plunge through a silicate magma ocean and do not emulsify entirely by turbulent erosion. This effect, in combination with the moderate W partition coefficient and metal/silicate ratio of mixing material of order unity ($K_W \cdot m_{impactor}/m_{target} \sim 1$), means that the Moon forming event had limited ability to re-equilibrate the entire mantle. The ε_W value of silicate Earth is thus linked to earlier events rather than the last giant impact, from which the Moon formed.

Acknowledgements

We thank Robin Canup for supporting data and helpful guidance through the interpretation of her SPH results. H. Schmeling and an anonymous reviewer greatly improved the manuscript. TWD thanks Peter D. Ditlevsen, Kaveh Pahlevan, Andy Knoll, and Minik T. Rosing for their comments, motivation, and fruitful discussions. We are thankful to our sponsors Danmarks Grundforskningsfond (Nordic Center for Earth Evolution), and Caltech SURF fellowship (TWD).

Appendix A. Supplementary data

Supplementary data associated with this article can be found, in the online version, at doi:10.1016/j.epsl.2010.03.038.

References

Allegre, C.J., Manhes, G., Gopel, C., 2008. The major differentiation of the Earth at similar to 4.45 Ga. Earth Planet. Sci. Lett. 267, 386–398.
Cameron, A.G.W., Benz, W., 1991. The origin of the moon and the single impact hypothesis-IV. Icarus 92, 204–216.
Canup, R.M., 2004. Simulations of a late lunar-forming impact. Icarus 168, 433–456.
Chambers, J.E., 2004. Planetary accretion in the inner solar system. Earth Planet. Sci. Lett. 223, 241–252.
Chandrasekhar, S., 1961a. Hydrodynamics and hydromagnetic stability. Oxford University Press.
Chandrasekhar, S., 1961b. Hydrodynamics and hydromagnetic stability. Oxford University Press. 447 pp.
Chandrasekhar, S., 1961c. Hydrodynamics and hydromagnetic stability. Oxford University Press. 481ff pp.
Chen, J.H.W., Wasserburg, G.J., 1996. Live 107Pd in the early solar system and implication for planetary evolution, earth processes: reading the isotopic code. Am. Geophys. Union 1–20.
Dalziel, S.B., Linden, P.F., Youngs, D.L., 1999. Self-similarity and internal structure of turbulence induced by Rayleigh–Taylor instability. J. Fluid Mech. 399, 1–48.
Davies, G.F., 1985. Heat deposition and retention in a solid planet growing by impacts. Icarus 63, 45–68.
Drake, M.J., Righter, K., 2002. Determining the composition of the Earth. Nature 416, 39–44.
Golabek, G.J., Schmeling, H., Tackley, P.J., 2008. Earth's core formation aided by flow channelling instabilities induced by iron diapirs. Earth Planet. Sci. Lett. 271, 24–33.
Halliday, A.N., 2004. Mixing, volatile loss and compositional change during impact-driven accretion of the Earth. Nature 427, 505–509.
Halliday, A.N., Lee, D.C., 1999. Tungsten isotopes and the early development of the Earth and Moon. Geochim. Cosmochim. Acta 63, 4157–4179.
Halliday, A., Rehkamper, M., Lee, D.C., Yi, W., 1996. Early evolution of the Earth and Moon: new constraints from Hf–W isotope geochemistry. Earth Planet. Sci. Lett. 142, 75–89.
Harper, C.L., Jacobsen, S.B., 1996. Evidence for Hf-182 in the early solar system and constraints on the timescale of terrestrial accretion and core formation. Geochim. Cosmochim. Acta 60, 1131–1153.
Ivanov, B.A., Neukum, G., Bottke, W.F., Hartmann, W.K., 2002. The comparison of size-frequency distributions of impact craters and asteroids and the planetary cratering rate. In: Bottke, A.C.W.F., Paolicchi, P., Binzel, R. (Eds.), Asteroids III. U. Arizona Press, pp. 89–101.
Jacobsen, S.B., 2005. The Hf–wisotopic system and the origin of the earth and moon. Ann. Rev. Earth Planet. Sci. 33, 531–570.
Jacobsen, S., Ranen, M., Petaev, M., Remo, J., O'Connell, R., Sasselov, D., 2008. Isotopes as clues to the origin and earliest differentiation history of the Earth. Philos. Trans. A 366, 4129.
Kleine, T., Munker, C., Mezger, K., Palme, H., 2002. Rapid accretion and early core formation on asteroids and the terrestrial planets from Hf–W chronometry. Nature 418, 952–955.
Kleine, T., Mezger, K., Palme, H., Munker, C., 2004. The W isotope evolution of the bulk silicate Earth: constraints on the timing and mechanisms of core formation and accretion. Earth Planet. Sci. Lett. 228, 109–123.
Kleine, T., Palme, H., Mezger, M., Halliday, A.N., 2005a. Hf–W chronometry of lunar metals and the age and early differentiation of the Moon. Science 310, 1671–1674.
Kleine, T., Mezger, K., Palme, H., Scherer, E., Munker, C., 2005b. The W isotope composition of eucrite metals: constraints on the timing and cause of the thermal metamorphism of basaltic eucrites. Earth Planet. Sci. Lett. 231, 41–52.

Kleine, T., Touboul, M., Bourdon, B., Nimmo, F., Mezger, K., Palme, H., Jacobsen, S.B., Yin, Q.-Z., Halliday, A.N., 2009. Hf–W chronology of the accretion and early evolution of asteroids and terrestrial planets. Geochim. Cosmochim. Acta 73, 5150–5188.
Kortenkamp, S.J., Wetherill, G.W., Inaba, S., 2001. Runaway growth of planetary embryos facilitated by massive bodies in a protoplanetary disk. Science 293, 1127–1129.
Kotsovinos, N.E., 1990. Dissipation of turbulent kinetic-energy in buoyant free shear flows. Int. J. Heat Mass Transf. 33, 393–400.
Lee, D.C., Halliday, A.N., 1996. Hf–W isotopic evidence for rapid accretion and differentiation in the early solar system. Science 274, 1876–1879.
Markowski, A., Quitte, G., Halliday, A.N., Kleine, T., 2006. Tungsten isotopic compositions of iron meteorites: chronological constraints vs. cosmogenic effects. Earth Planet. Sci. Lett. 242, 1–15.
McDonough, W.F., 2003. Compositional model for the Earth's core. Treatise on Geochemistry, 2, pp. 547–568.
Melosh, H.J., 1990. Impact Cratering — A Geological Process. Oxford University Press.
Morton, B.R., Taylor, G., Turner, J.S., 1956. Turbulent gravitational convection from maintained and instantaneous sources. Proc. R. Soc. Lond. A Math. Phys. Sci. 234, 1–23.
Nimmo, F., Kleine, T., 2007. How rapidly did Mars accrete? Uncertainties in the Hf–W timing of core formation. Icarus 191, 497–504.
O'Brien, D.P., Morbidelli, A., Levison, H.F., 2006. Terrestrial planet formation with strong dynamical friction. Icarus 184, 39–58.
Ogihara, M., Ida, S., Morbidelli, A., 2007. Accretion of terrestrial planets from oligarchs in a turbulent disk. Icarus 188, 522–534.
Okamoto, M., 1996. Theoretical modelling of buoyancy-driven turbulent flows. J. Phys. Soc. Jpn 65, 2044–2059.
Papanicolaou, P.N., List, E.J., 1988. Investigations of round vertical turbulent buoyant jets. J. Fluid Mech. 195, 341–391.
Petaev, M., Jacobsen, S., Remo, J., Adams, R., Sasselov, D., 2008. Experimental Study of High-Energy Processing of Protoplanetary Materials. LPS 39, #1850.
Porcelli, D., Woolum, D., Cassen, P., 2001. Deep Earth rare gases: initial inventories, capture from the solar nebula, and losses during Moon formation. Earth Planet. Sci. Lett. 193, 237–251.
Righter, K., Drake, M.J., Yaxley, G., 1997. Prediction of siderophile element metal–silicate partition coefficients to 20 GPa and 2800 degrees C: the effects of pressure, temperature, oxygen fugacity, and silicate and metallic melt compositions. Phys. Earth Planet. Inter. 100, 115–134.
Rubie, D.C., Melosh, H.J., Reid, J.E., Liebske, C., Righter, K., 2003. Mechanisms of metal–silicate equilibration in the terrestrial magma ocean. Earth Planet. Sci. Lett. 205, 239–255.
Sasaki, T., Abe, Y., 2007. Rayleigh–Taylor instability after giant impacts: imperfect equilibration of the Hf–W system and its effect on the core formation age. Earth Planets Space 59, 1035–1045.
Schoenberg, R., Kamber, B.S., Collerson, K.D., Eugster, O., 2002. New W-isotope evidence for rapid terrestrial accretion and very early core formation. Geochim. Cosmochim. Acta 66, 3151–3160.
Smyth, W.D., Moum, J.N., 2000. Length scales of turbulence in stably stratified mixing layers. Phys. Fluids 12, 1327–1342.
Smyth, W.D., Moum, J.N., Caldwell, D.R., 2001. The efficiency of mixing in turbulent patches: inferences from direct simulations and microstructure observations. J. Phys. Oceanogr. 31, 1969–1992.
Snider, D., Andrews, M., 1994. Rayleigh–Taylor and shear driven mixing with an unstable thermal stratification. Phys. Fluids 6, 3324.
Stevenson, D.J., 1990. Fluid dynamics and core formation. In: Jones, H.E.N.a.J.H. (Ed.), Origin of the Earth. Oxford University Press, New York, pp. 231–250.
Tennekes, H.L.J., 1972. A first Course in Turbulence. MIT press.
Tera, F., Papanastassiou, D.A., Wasserburg, G.J, 1974. Isotopic evidence for a terminal lunar cataclysm. Earth Planet. Sci. Lett. 22, 1–21.
Tonks, W.B., Melosh, H.J., 1993. Magma ocean formation due to giant impacts. J. Geophys. Res.-Planets 98, 5319–5333.
Touboul, M., Kleine, T., Bourdon, B., Palme, H., Wieler, R., 2007. Late formation and prolonged differentiation of the Moon inferred from W isotopes in lunar metals. Nature 450, 1206–1209.
Tschauner, O., Willis, M., Asimow, P., Ahrens T., 2005. Effective liquid metal–silicate mixing upon shock by power–law droplet size scaling in Richtmyer–Meshkov like perturbations. LPS 36, #1802.
Turner, J.S., 1986. Turbulent entrainment — the development of the entrainment assumption, and its application to geophysical flows. J. Fluid Mech. 173, 431–471.
Weidenschilling, S.J., 2000. Formation of planetesimals and accretion of the terrestrial planets. Kluwer Academic Publ, pp. 295–310.
Wood, B.J., Halliday, A.N., 2005. Cooling of the Earth and core formation after the giant impact. Nature 437, 1345–1348.
Yin, Q.Z., Jacobsen, S.B., Yamashita, K., Blichert-Toft, J., Telouk, P., Albarede, F., 2002. A short timescale for terrestrial planet formation from Hf–W chronometry of meteorites. Nature 418, 949–952.